

## Satellite-based constraints on explosive SO<sub>2</sub> release from Soufrière Hills Volcano, Montserrat

Simon A. Carn<sup>1</sup> and Fred J. Prata<sup>2</sup>

Received 2 August 2010; accepted 12 August 2010; published 18 September 2010.

[1] Numerous episodes of explosive degassing have punctuated the 1995–2009 eruption of Soufrière Hills volcano (SHV), Montserrat, often following major lava dome collapses. We use ultraviolet (UV) and infrared (IR) satellite measurements to quantify sulfur dioxide (SO<sub>2</sub>) released by explosive degassing, which is not captured by routine ground-based and airborne gas monitoring. We find a total explosive SO<sub>2</sub> release of ~0.5 Tg, which represents ~6% of total SO<sub>2</sub> emissions from SHV since July 1995. The majority of this SO<sub>2</sub> (~0.4 Tg) was vented following the most voluminous SHV dome collapses in July 2003 and May 2006. Based on our analysis, we suggest that the SO<sub>2</sub> burden measured following explosive disruption of lava domes depends on several factors, including the instantaneous lava effusion rate, dome height above the conduit, and the vertical component of directed explosions. Space-based SO<sub>2</sub> measurements merit inclusion in routine gas monitoring at SHV and other dome-forming volcanoes. **Citation:** Carn, S. A., and F. J. Prata (2010), Satellite-based constraints on explosive SO<sub>2</sub> release from Soufrière Hills Volcano, Montserrat, *Geophys. Res. Lett.*, 37, L00E22, doi:10.1029/2010GL044971.

### 1. Introduction

[2] Explosive activity is among the most common and hazardous features of lava dome eruptions [Newhall and Melson, 1983]. During lava dome extrusion, strong pressure gradients develop at the conduit head and within the dome due to degassing and crystallization of ascending magma [Sparks, 1997]. The resulting viscous lava dome modulates gas flow from depth and supports high interior gas pressures that can initiate dome collapse [Voight and Elsworth, 2000] or dissipation of overpressure through forceful expulsion of gases and volcanic ash (ash venting) [e.g., Edmonds and Herd, 2007]. Removal of overburden during a lava dome collapse exposes the overpressured dome interior and conduit, and can trigger violent explosive eruptions.

[3] The 1995–2009 eruption of Soufrière Hills Volcano (SHV), Montserrat has been punctuated by numerous episodes of explosive activity, usually following large lava dome collapses (LDCs) [e.g., Herd et al., 2005; Prata et al., 2007]. Intense rainfall has often been implicated as a trigger mechanism in these LDCs [e.g., Matthews et al., 2002]. The

tendency of SHV to purge most of its lava dome in short-duration LDCs [e.g., Herd et al., 2005] distinguishes it from other dome-forming volcanoes. Eruption columns generated by explosive degassing at SHV have reached the stratosphere [Prata et al., 2007] and constitute a significant aviation hazard. However, the typical degassing regime at SHV, regardless of whether lava is extruding, has been continuous gas emissions entrained in a lower tropospheric plume at ~1 km altitude.

[4] Persistent sulfur dioxide (SO<sub>2</sub>) emissions from SHV are sustained by a relatively constant supply of volatiles from degassing of deep mafic magma [Edmonds et al., 2003; Christopher et al., 2010]. This gas ascends through permeable bubble and fracture networks, and discharges predominantly along conduit margins where shear-induced fragmentation promotes gas release. Monitoring of SO<sub>2</sub> output thus elucidates the deep supply of mafic magma to the system, and hence eruption cycling [Elsworth et al., 2008]. SO<sub>2</sub> emission rates have been monitored throughout the eruption via correlation spectroscopy (COSPEC) and, since January 2002, using an array of scanning ultraviolet (UV) spectrometers [Christopher et al., 2010]. However, explosive degassing events are rarely captured by the spectrometer array [Christopher et al., 2010], which is aligned to measure the tropospheric plume transported west of SHV by easterly trade winds.

[5] We report here a complete time-series of satellite measurements of explosive SO<sub>2</sub> emissions from SHV, which complements the ground-based data and further constrains the total sulfur (S) budget of the eruption. Our analysis includes all significant explosive events from the SHV dome since July 1995, including explosions triggered by or closely associated with LDCs. Our results permit assessment of SO<sub>2</sub> partitioning between passive and explosive degassing, and are also relevant to studies of the possible climate impacts of long-term lava dome eruptions.

### 2. Satellite data

[6] The satellite SO<sub>2</sub> measurements employed here originate from five space-borne instruments spanning UV to thermal infrared (TIR) wavelengths (Table 1). The SHV eruption straddles a major improvement in satellite sensitivity to SO<sub>2</sub>. TOMS measurements were restricted to SO<sub>2</sub> loadings of ~4 kt or more in the upper troposphere and lower stratosphere (UTLS) [Krueger et al., 2000; Carn et al., 2003], whereas OMI can detect passive volcanic degassing on a daily basis [Carn et al., 2008]. The NASA Afternoon Constellation or ‘A-Train’ now permits improved synergy between multi-spectral measurements of volcanic clouds [e.g., Prata et al., 2007; Carn et al., 2009].

[7] OMI SO<sub>2</sub> retrievals reported here are derived from the operational algorithm [Yang et al., 2007], and require an

<sup>1</sup>Department of Geological and Mining Engineering and Sciences, Michigan Technological University, Houghton, Michigan, USA.

<sup>2</sup>Atmosphere and Climate Department, Norwegian Institute for Air Research, Kjeller, Norway.

**Table 1.** Satellite Sensors Used to Measure SO<sub>2</sub> Emissions From SHV, 1995–2009

Instrument <sup>a</sup>	Satellite(s)	Operational Lifetime	Equator Crossing (Local Time)	Spectral Coverage	Spatial Resolution (nadir, km)	SO <sub>2</sub> Retrieval Precision <sup>b</sup>		Reference <sup>c</sup>
						Single Pixel (DU)	Minimum SO <sub>2</sub> Mass (tons)	
TOMS	Earth Probe	7/1996–12/2005	1100–1130	UV, 6 bands	39×39	18	3800	1
MODIS	Terra, Aqua	2/2000–(Terra) 7/2002–(Aqua) 7/2002–	1030 (Terra) 1330 (Aqua)	Vis-TIR, 36 bands	1×1	26	20	2
AIRS	Aqua	7/2002–	1330	TIR, hyperspectral	13.5 (circular)	6	120	3
SEVIRI	MSG <sup>d</sup>	1/2004–	Geostationary at 3°W	Vis-TIR, 12 bands	5×5	10	35	4
OMI	Aura	9/2004–	1345	UV-Vis, hyperspectral	13×24	1	45	5

<sup>a</sup>TOMS, Total Ozone Mapping Spectrometer; MODIS, Moderate Resolution Imaging Spectroradiometer; AIRS, Atmospheric Infrared Sounder; SEVIRI, Spinning Enhanced Visible and Infrared Imager; OMI, Ozone Monitoring Instrument.

<sup>b</sup>Given in terms of SO<sub>2</sub> column amount in a single nadir pixel (in Dobson Units [DU] where 1 DU = 0.0285 g m<sup>-2</sup> SO<sub>2</sub>) and as the estimated minimum detectable SO<sub>2</sub> mass (for a cloud covering 5 contiguous pixels) under cloud-free conditions in the UTLS.

<sup>c</sup>1, *Krueger et al.* [2000]; 2, *Prata et al.* [2003]; 3, *Prata and Bernardo* [2007]; 4, *Prata and Kerkmann* [2007]; 5, *Yang et al.* [2007].

<sup>d</sup>Meteosat Second Generation.

estimate of SO<sub>2</sub> cloud center of mass altitude (CMA). Independent estimates of cloud altitude (Table 2) have been used to select the appropriate CMA, which was typically in the mid-troposphere (CMA = 7.5 km) or lower stratosphere (CMA = 17.5 km). The overall uncertainty on the OMI SO<sub>2</sub> retrievals (including CMA errors) for SO<sub>2</sub> clouds above 5 km altitude is ~20% [*Yang et al.*, 2007]. *Prata and Bernardo* [2007] describe an AIRS SO<sub>2</sub> retrieval scheme that exploits the strong  $\nu_3$  SO<sub>2</sub> absorption band centered at 7.3  $\mu\text{m}$ . MODIS SO<sub>2</sub> retrievals also utilize this waveband, albeit with lower spectral resolution and higher spatial resolution than AIRS, using a similar technique to that described by *Prata et al.* [2003]. SO<sub>2</sub> measurements with 15-minute temporal resolution are also possible using the geostationary SEVIRI instrument [*Prata and Kerkmann*, 2007]. We caution that most of these SO<sub>2</sub> measurements have not been rigorously validated for a range of atmospheric conditions. Limited validation of TOMS SO<sub>2</sub> data was achieved [*Krueger et al.*, 2000], and early efforts to validate OMI SO<sub>2</sub> columns have been successful [*Spinei et al.*, 2010].

[8] Various geophysical factors affect the sensitivity of UV and IR SO<sub>2</sub> retrievals. The former depend on total column ozone, solar zenith and viewing zenith angles, surface reflectivity, meteorological cloud fraction and altitude, and aerosol abundance. In the IR, plume transparency, thermal contrast (between the SO<sub>2</sub> layer and subjacent IR emission source) and water vapor (H<sub>2</sub>O) are critical factors. Accurate OMI retrievals are possible if a realistic SO<sub>2</sub> CMA is specified in the algorithm [*Yang et al.*, 2007]. Our IR SO<sub>2</sub> retrievals using the  $\nu_3$  SO<sub>2</sub> waveband (in a region of strong H<sub>2</sub>O absorption) are only sensitive to SO<sub>2</sub> located above the bulk of the H<sub>2</sub>O column. The precise cutoff altitude depends on the H<sub>2</sub>O vertical profile and can be computed using radiosonde soundings [*Prata et al.*, 2007], but typically ranges from ~2–5 km. Estimates of SO<sub>2</sub> retrieval precision are provided in Table 1.

[9] Any S species other than SO<sub>2</sub> (e.g., H<sub>2</sub>S) would not be detected from space. SHV also emits significant HCl during active dome growth [*Christopher et al.*, 2010]. Lower tropospheric HCl cannot be measured from space, but the Microwave Limb Sounder (MLS) on Aura retrieves vertical profiles of HCl mixing ratio in the UTLS and detected HCl from SHV in May 2006. MLS has poor spatial coverage but *Prata et al.* [2007] report an HCl/SO<sub>2</sub> ratio of 0.03–0.1 and ~3–10 kt of HCl based on MLS and AIRS data. In comparison, HCl/SO<sub>2</sub> molar ratios in SHV's tropospheric plume are <0.5 during eruption pauses, but up to ~7 during active dome growth [*Christopher et al.*, 2010]. The discrepancy between these ratios likely reflects a combination of the poor spatial sampling of MLS, differences in HCl/SO<sub>2</sub> ratios between passively and explosively degassed volatiles, and perhaps preferential scavenging of HCl by hydrometeors in explosive eruption columns.

### 3. Results

[10] We have analyzed satellite data for the largest LDCs and explosive events at SHV since 1995, and report the maximum SO<sub>2</sub> loadings derived from each sensor in Table 2 and Figure 1. Near-coincident measurements derived from the UV and IR sensors are generally in good agreement (Table 2), providing confidence in the retrieval techniques. MODIS appears less sensitive to SO<sub>2</sub> than AIRS for simul-

**Table 2.** Satellite Measurements of SO<sub>2</sub> Emissions Associated with LDCs and Explosive Events at SHV

Explosion/Collapse Time <sup>a</sup> (UT)	Collapse + Tephra Volume <sup>b</sup> (Mm <sup>3</sup> )	Satellite Overpass (UT)	Measured SO <sub>2</sub> Emission (Gg)	Plume Altitude <sup>c</sup> (km)	Extrusion Hiatus <sup>d</sup> (days)
26 Dec 1997, 07:00	46	EP TOMS (15:43)	31.0 <sup>e</sup>	15	0
3 July 1998, 07:02	16 (R)	EP TOMS (14:47)	5.0	9–12	NDG
12 Nov 1998, 10:07	2.5	EP TOMS (15:31)	9.0	8	NDG
20 July 1999	4.2	EP TOMS (15:48)	16.0	11	NDG
20 Mar 2000, 23:23	23 (NP, R)	Terra MODIS (21 Mar, 02:00)	3.4	9	4
29 Jul 2001, 23:50	36.5 (P, R)	EP TOMS (30 Jul, 15:58)	33.0	11	4
		Terra MODIS (30 Jul, 15:45)	33.6		
13 Jul 2003, 03:35	135 (P, R)	EP TOMS (14:21)	100	15	8–15
		Aqua MODIS (16:55)	128		
		AIRS (16:55)	123		
28 Jun 2005, 17:06	Explosion (NP)	OMI (17:36)	1.0	7	NDG
3 Jul 2005, 05:30	Explosion (NP)	OMI (17:55)	4.0		NDG
18 Jul 2005, 07:01	Explosion	OMI (17:12)	3.0	>6	NDG
20 May 2006, 11:00	83 (P, R)	SEVIRI (06:15 May 21)	178	20	0.3
		Aqua MODIS (06:35 May 21)	123		
		AIRS (06:35 May 21)	233		
		OMI (17:32 May 21)	220		
8 Jan 2007, 09:30	<1; Explosion, PF	OMI (16:57)	1.0	9	-
29 Jul 2008, 03:28	1.3; Explosions, PFs, pumice fall (P)	OMI (17:40)	3.0	12	4–11
3 Dec 2008, 02:35	Explosions, PFs, ballistics (NP)	AIRS (05:55)	7.1	~13	7
		Aqua MODIS (05:55)	6.0		
		OMI (18:35)	7.0		
3 Jan 2009, 08:47, 11:07	1.3; Explosions, column collapse (P)	Aqua MODIS (17:45)	8.0	~11	-
		OMI (17:54)	0.5 <sup>e</sup>		

<sup>a</sup>From MVO (<http://www.mvo.ms>) and Smithsonian Institution (SI) reports (<http://www.volcano.si.edu/world/volcano.cfm?vnum=1600-05>).

<sup>b</sup>All volumes as dense rock equivalent (DRE; Mm<sup>3</sup> = 10<sup>6</sup> m<sup>3</sup>). Sources: *Norton et al.* [2002], *Herd et al.* [2005], and *Wadge et al.* [2010]. Volumes for explosive events are typically unknown. *P*, pumice found in deposits; *NP*, pumice absent; *R*, intense rainfall prior to or during event. *PF*, pyroclastic flow.

<sup>c</sup>From SI reports (see above) and *Wadge et al.* [2010].

<sup>d</sup>Delay until resumption of dome growth (if known) [following *Wadge et al.*, 2010]; NDG, no dome growth.

<sup>e</sup>Incomplete coverage of SO<sub>2</sub> cloud: minimum value.

taneous measurements, probably due to the lower MODIS spectral resolution. Summing the maximum loading for each event, we obtain a total explosive SO<sub>2</sub> emission of ~0.5 Tg, of which ~0.4 Tg was released during the two largest LDCs (13 July 2003, 20 May 2006). *Christopher et al.* [2010] report a total cumulative S emission of ~3.5 Tg for the eruption through mid-2009, based on ground-based measurements. Incorporating our data yields a combined total S emission of 3.74 Tg through January 2009, of which ~6% is derived from explosive degassing.

[11] Removal of SO<sub>2</sub> by conversion to sulfate aerosol and wet and dry deposition occurs in the interval between SO<sub>2</sub> release and the satellite overpass time. For the SHV events (Table 2), this time delay varies from ~0.5–20 hours; adjusting the SO<sub>2</sub> loadings using a 30% day<sup>-1</sup> SO<sub>2</sub> loss rate (high for the UTLS) has no significant impact on our results. SO<sub>2</sub> measurements are also affected by volcanic ash, which violates retrieval assumptions, impacts plume opacity, and may also scavenge SO<sub>2</sub>. We have not corrected for these effects, but note that ash abundances were low in most of the SO<sub>2</sub> clouds studied at the time measurements were made. Finally, as noted above, several LDCs coincided with intense rainfall (Table 2), which may have sequestered some SO<sub>2</sub> (and other soluble gases). This is not explored further here.

[12] No measurable SO<sub>2</sub> was produced by LDCs early in the SHV eruption (1996–1997). *Carn et al.* [2003] note low SO<sub>2</sub> emissions associated with Vulcanian explosions in August–October 1997. Since the ascending magma degasses most of its sulfur at depth (>6 km) [*Edmonds et al.*, 2003], this may reflect low conduit drawdown depths (0.5–2 km)

[*Druitt et al.*, 2002], which tapped relatively S-poor magma. Eruption of pumice (Table 2 and Figure 2) indicates involvement of juvenile magma from the conduit or dome interior; events producing pumice are associated with higher SO<sub>2</sub> emissions (Figure 2). Nevertheless, the March 1998–November 1999 eruptive pause also saw several significant explosive SO<sub>2</sub> emissions and elevated SO<sub>2</sub> emission rates

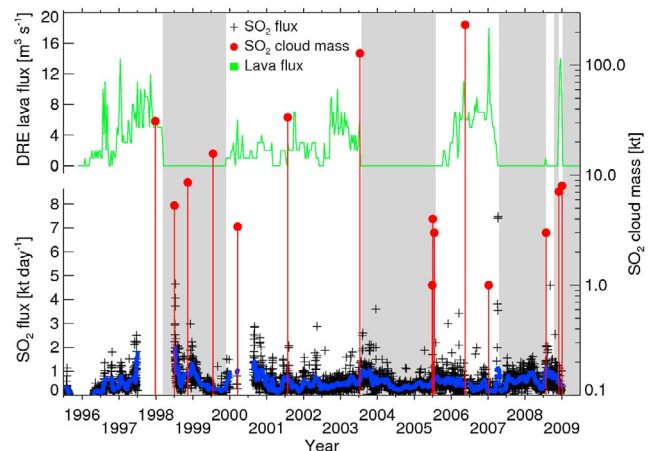


**Figure 1.** Satellite-derived SO<sub>2</sub> cloud burdens plotted with ground-based SO<sub>2</sub> emission rate data [*Christopher et al.*, 2010] and DRE lava volume flux [*Wadge et al.*, 2010] for the 1995–2009 SHV eruption. Blue symbols show a 4-week running mean of the SO<sub>2</sub> emission rates. Gray bands demarcate periods of lava dome stagnation [*Wadge et al.*, 2010].

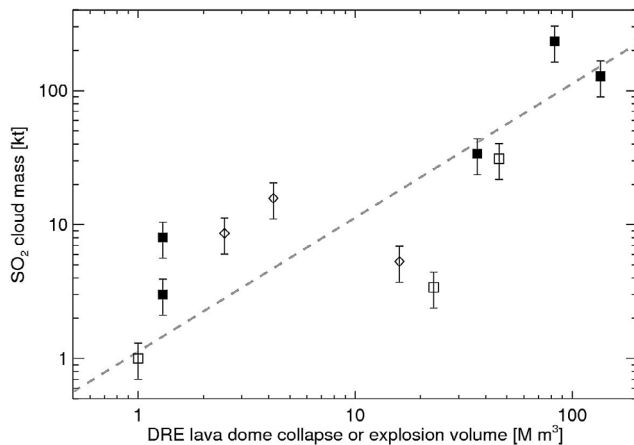


**Figure 2.** Explosive SO<sub>2</sub> emissions against DRE lava volume flux [Wadge *et al.*, 2010]. *Black/open symbols* are satellite SO<sub>2</sub> measurements (with 30% error bars) for events with/without reported pumice in the deposits. *Squares/diamonds* indicate events during active extrusion/eruption pauses. The *dashed line* indicates the theoretical maximum SO<sub>2</sub> yield from the collapsed dome volume, assuming complete degassing of andesite with density 2250 kg m<sup>-3</sup> (core lava density from Wadge *et al.* [2010]) and containing 250 ppm S (the S content of melt inclusions in plagioclase phenocrysts in the erupted andesite) [Christopher *et al.*, 2010].

(Figure 1), indicating a sustained supply of SO<sub>2</sub> from depth that may have played a role in triggering these LDCs.

[13] We note a tendency for higher explosive SO<sub>2</sub> emissions during active dome growth, and a broad correlation between SO<sub>2</sub> release and LDC or explosion volume (Figures 1 and 2; note that collapse volumes do not include distal fine ash deposits). Many events appear to require more SO<sub>2</sub> than is potentially available through degassing of interstitial melt in the collapsed lava volume (Figure 2). Possible sources of this ‘excess’ gas include (1) an SO<sub>2</sub>-rich volatile phase trapped within fractures in the dome, released during collapse; (2) syn-LDC degassing of fresh magma rising in the conduit (a source of pumice); and (3) gas extracted from within fractures and permeable networks in the upper part of the volcanic edifice. Liberation of SO<sub>2</sub> via (2) and (3) will depend on the magnitude and timescale of overburden removal during a LDC, which will in turn be controlled by the elevation of the dome prior to collapse and dome growth history in the preceding weeks or months.

#### 4. Discussion and Concluding Remarks

[14] The observation that LDCs during active dome growth produce higher SO<sub>2</sub> emissions implicates relatively fresh dome or conduit magma as an important gas source during these events. It is more likely to degas explosively on decompression than older, degassed dome lava. Furthermore, high effusion rates during a collapse would promote shear-induced fragmentation and gas release along conduit margins. We also note that LDCs during active growth tend to precede a reduction in SO<sub>2</sub> emission rates (e.g., after 20 May 2006, they dropped below the long-term eruption average), whereas

LDCs during eruptive pauses or towards the end of dome growth phases trigger increased SO<sub>2</sub> emissions (Figure 1). Following surface unloading during the July 2003 collapse, Voight *et al.* [2006] attribute an overpressure increase of 1 MPa to the growth of 1–3% gas bubbles in a magma reservoir ~6 km below the crater, which could explain increased post-collapse SO<sub>2</sub> emissions (Figure 1). This contrasts with the May 2006 collapse, despite a similar magnitude of overburden removal. The state of the magma in the conduit (e.g., its viscosity profile) may impact its ability to transmit pressure changes to a deep reservoir.

[15] The 20 May 2006 collapse produced the largest SO<sub>2</sub> cloud of the SHV eruption to date; a ~0.2 Tg injection into the lower stratosphere that was tracked halfway around the globe [Prata *et al.*, 2007; Carn *et al.*, 2009], perturbing stratospheric aerosol abundance [Thomason and Pitts, 2008]. A unique combination of factors appears to be responsible for the high SO<sub>2</sub> release measured after this event. Of all the major LDCs, the May 2006 event uniquely satisfies three criteria shortly prior to or during the collapse: (1) a high lava extrusion rate (11–12 m<sup>3</sup> s<sup>-1</sup> (Figure 1)); (2) dome elevation >950 m [Wadge *et al.*, 2010]; and (3) a strong vertical component to the paroxysmal explosion (suggested by a column height of 20 km (Table 2)). The 26 Dec 1997 LDC also satisfies (1) and (2), but the paroxysmal event was a lateral blast. If the majority of the expelled volatiles are directed laterally, we posit that emitted SO<sub>2</sub> will reside at lower altitudes, disperse more rapidly, and that less will be measured from space (note also that the SO<sub>2</sub> yield for the 26 Dec 1997 LDC is a minimum value (Table 2)). The trajectory of directed explosions will depend on dome-core architecture (e.g., the orientation and cooling history of individual lobes) [e.g., Voight and Elsworth, 2000], and hence dome growth history, and the collapse style (e.g., piecemeal or catastrophic).

[16] However, our understanding of the source of SO<sub>2</sub> in explosive emissions from SHV remains incomplete. Evacuation of fresh conduit magma as pumice undoubtedly contributes a significant quantity of volatiles, though upper conduit magma is expected to be relatively SO<sub>2</sub>-poor. Cessation of dome growth for some time after a collapse suggests greater drawdown depths or stagnated magma in the conduit, yet dome growth recommenced <1 day after the 20 May 2006 collapse (Table 2). Refilling of a conduit with cross-sectional area 1000 m<sup>2</sup> [Edmonds *et al.*, 2003] evacuated to a depth of 2–5 km would take ~2–6 days at an extrusion rate of 10 m<sup>3</sup> s<sup>-1</sup>. In such cases, perhaps the conduit is only partially evacuated (only the hotter, more volatile-rich fraction), leaving remnant lava that extrudes as apparent ‘new’ growth soon afterwards.

[17] To conclude, we stress the increasing utility of satellite measurements for monitoring degassing volcanoes and for constraining the total S budget of eruptions. OMI has sufficient sensitivity to monitor the SHV SO<sub>2</sub> plume on a regular basis, and has detected many episodes of ash and gas venting not discussed here. Relatively minor SO<sub>2</sub> emissions (e.g., June–July 2005 (Table 2)) may signify rising batches of new magma and changes in permeability; quantification of such emissions is thus beneficial to monitoring efforts. Satellite surveillance of SHV becomes vital when the UV spectrometer network malfunctions, or when plume dispersion is atypical. A combination of UV and IR sensors provides optimal coverage for monitoring volcanic SO<sub>2</sub> emissions.

[18] **Acknowledgments.** Funding for this work was provided by NASA (grant NNX09AJ40G to SAC). We thank two anonymous referees for comments that significantly improved the paper.

## References

- Carn, S. A., A. J. Krueger, G. J. S. Bluth, S. J. Schaefer, N. A. Krotkov, I. M. Watson, and S. Datta (2003), Volcanic eruption detection by the Total Ozone Mapping Spectrometer (TOMS) instruments: A 22-year record of sulfur dioxide and ash emissions, in *Volcanic Degassing*, edited by C. Oppenheimer, D. M. Pyle, and J. Barclay, *Spec. Publ. Geol. Soc. London*, 213, 77–202.
- Carn, S. A., A. J. Krueger, N. A. Krotkov, S. Arellano, and K. Yang (2008), Daily monitoring of Ecuadorian volcanic degassing from space, *J. Volcanol. Geotherm. Res.*, 176, 141–150, doi:10.1016/j.jvolgeores.2008.01.029.
- Carn, S. A., A. J. Krueger, N. A. Krotkov, K. Yang, and K. Evans (2009), Tracking volcanic sulfur dioxide clouds for aviation hazard mitigation, *Nat. Hazards*, 51(2), 325–343, doi:10.1007/s11069-008-9228-4.
- Christopher, T., M. Edmonds, M. C. S. Humphreys, and R. A. Herd (2010), Volcanic gas emissions from Soufrière Hills Volcano, Montserrat 1995–2009 with implications for mafic magma supply and degassing, *Geophys. Res. Lett.*, 37, L00E04, doi:10.1029/2009GL041325.
- Druitt, T. H., et al. (2002), Periodic vulcanian explosions and fountain collapse at the Soufrière Hills Volcano, Montserrat, 1997, in *The Eruption of Soufrière Hills Volcano, Montserrat, From 1995 to 1999*, edited by T. H. Druitt and B. P. Kokelaar, *Geol. Soc. London Mem.*, 21, 281–306.
- Edmonds, M., and R. A. Herd (2007), A volcanic degassing event at the explosive-effusive transition, *Geophys. Res. Lett.*, 34, L21310, doi:10.1029/2007GL031379.
- Edmonds, M., C. Oppenheimer, D. M. Pyle, R. A. Herd, and G. Thompson (2003), SO<sub>2</sub> emissions from Soufrière Hills Volcano and their relationship to conduit permeability, hydrothermal interaction and degassing regime, *J. Volcanol. Geotherm. Res.*, 124, 23–43, doi:10.1016/S0377-0273(03)00041-6.
- Elsworth, D., G. Mattioli, J. Taron, B. Voight, and R. Herd (2008), Implications of magma transfer between multiple reservoirs on eruption cycling, *Science*, 322, 246–248, doi:10.1126/science.1161297.
- Herd, R. A., M. Edmonds, and V. A. Bass (2005), Catastrophic lava dome failure at Soufrière Hills Volcano, Montserrat, 12–13 July 2003, *J. Volcanol. Geotherm. Res.*, 148, 234–252, doi:10.1016/j.jvolgeores.2005.05.003.
- Krueger, A. J., S. Schaefer, N. Krotkov, G. Bluth, and S. Barker (2000), Ultraviolet remote sensing of volcanic emissions, in *Remote Sensing of Active Volcanism*, *Geophys. Monogr. Ser.*, vol. 116, edited by P. J. Mouginis-Mark et al., pp. 25–43, AGU, Washington, D. C.
- Mathews, A. J., J. Barclay, S. Carn, G. Thompson, J. Alexander, R. Herd, and C. Williams (2002), Rainfall induced volcanic activity on Montserrat, *Geophys. Res. Lett.*, 29(13), 1644, doi:10.1029/2002GL014863.
- Newhall, C. G., and W. G. Melson (1983), Explosive activity associated with the growth of volcanic domes, *J. Volcanol. Geotherm. Res.*, 17, 111–131, doi:10.1016/0377-0273(83)90064-1.
- Norton, G. E., et al. (2002), Pyroclastic flow and explosive activity at Soufrière Hills Volcano, Montserrat, during a period of virtually no magma extrusion (March 1998 to November 1999), in *The Eruption of Soufrière Hills Volcano, Montserrat, From 1995 to 1999*, edited by T. H. Druitt and B. P. Kokelaar, *Geol. Soc. London Mem.*, 21, 467–482.
- Prata, A. J., and C. Bernardo (2007), Retrieval of volcanic SO<sub>2</sub> column abundance from Atmospheric Infrared Sounder data, *J. Geophys. Res.*, 112, D20204, doi:10.1029/2006JD007955.
- Prata, A. J., and J. Kerkmann (2007), Simultaneous retrieval of volcanic ash and SO<sub>2</sub> using MSG-SEVIRI measurements, *Geophys. Res. Lett.*, 34, L05813, doi:10.1029/2006GL028691.
- Prata, A. J., W. I. Rose, S. Self, and D. M. O'Brien (2003), Global, long-term sulphur dioxide measurements from TOVS data: A new tool for studying explosive volcanism and climate, in *Volcanism and the Earth's Atmosphere*, *Geophys. Monogr. Ser.*, vol. 139, edited by A. Robock and C. Oppenheimer, pp. 75–92, AGU, Washington, DC.
- Prata, A. J., S. A. Carn, A. Stohl, and J. Kerkmann (2007), Long range transport and fate of a stratospheric volcanic cloud from Soufrière Hills Volcano, Montserrat, *Atmos. Chem. Phys.*, 7, 5093–5103, doi:10.5194/acp-7-5093-2007.
- Sparks, R. S. J. (1997), Causes and consequences of pressurization in lava dome eruptions, *Earth Planet. Sci. Lett.*, 150, 177–189, doi:10.1016/S0012-821X(97)00109-X.
- Spinei, E., S. A. Carn, N. A. Krotkov, G. H. Mount, K. Yang, and A. J. Krueger (2010), Validation of OMI SO<sub>2</sub> measurements in the Okmok volcanic cloud over Pullman, WA, July 2008, *J. Geophys. Res.*, doi:10.1029/2009JD013492, in press.
- Thomason, L. W., and M. C. Pitts (2008), CALIPSO observations of volcanic aerosol in the stratosphere, *Proc. SPIE*, 7153, 715300, doi:10.1117/12.804090.
- Voight, B., and D. Elsworth (2000), Instability and collapse of hazardous gas-pressurized lava domes, *Geophys. Res. Lett.*, 27(1), 1–4, doi:10.1029/1999GL008389.
- Voight, B., et al. (2006), Unprecedented pressure increase in deep magma reservoir triggered by lava-dome collapse, *Geophys. Res. Lett.*, 33, L03312, doi:10.1029/2005GL024870.
- Wadge, G., R. Herd, G. Ryan, E. S. Calder, and J.-C. Komorowski (2010), Lava production at Soufrière Hills Volcano, Montserrat: 1995–2009, *Geophys. Res. Lett.*, 37, L00E03, doi:10.1029/2009GL041466.
- Yang, K., N. A. Krotkov, A. J. Krueger, S. A. Carn, P. K. Bhartiya, and P. F. Levelt (2007), Retrieval of large volcanic SO<sub>2</sub> columns from the Aura Ozone Monitoring Instrument (OMI): Comparison and limitations, *J. Geophys. Res.*, 112, D24S43, doi:10.1029/2007JD008825.

S. A. Carn, Department of Geological and Mining Engineering and Sciences, Michigan Technological University, 1400 Townsend Dr., Houghton, MI 49931, USA. (scarn@mtu.edu)

F. J. Prata, Atmosphere and Climate Department, Norwegian Institute for Air Research, Instituttveien 18, N-2027 Kjeller, Norway. (fred.prata@nilu.no)